

Learning Partial Differential Equations with Deep Parallel Neural Operators

Qinglong Ma^a, Peizhi Zhao^a, Sen Wang^a, Tao Song^{a,*}

^a*College of Computer Science and Technology, China University of Petroleum (East China), Qingdao, 266580, Shandong, China*

Abstract

In recent years, Solving partial differential equations has shifted the focus of traditional neural network studies from finite-dimensional Euclidean spaces to generalized functional spaces in research. A novel methodology is to learn an operator as a means of approximating the mapping between outputs. Currently, researchers have proposed a variety of operator architectures. Nevertheless, the majority of these architectures adopt an iterative update architecture, whereby a single operator is learned from the same function space. In practical physical science problems, the numerical solutions of partial differential equations are complex, and a serial single operator is unable to accurately approximate the intricate mapping between input and output. So, We propose a deep parallel operator model (DPNO) for efficiently and accurately solving partial differential equations. DPNO employs convolutional neural networks to extract local features and map data into distinct latent spaces. Designing a parallel block of double Fourier neural operators to solve the iterative error problem. DPNO approximates complex mappings between inputs and outputs by learning multiple operators in different potential spaces in parallel blocks. DPNO achieved the best performance on five of them, with an average improvement of 10.5%, and ranked second on one dataset.

Keywords: neural operator, scientific machine learning, deep learning-based PDE solver, neural network

*corresponding author

Email address: `tsong@upc.edu.cn` (Tao Song)

1. Introduction

In scientific and engineering fields, partial differential equations (PDEs) are commonly used to model phenomena in a variety of physical domains, such as fluid mechanics, mechanics of materials, quantum mechanics, and electricity. The vast majority of partial differential equations lack analytical solutions, such as the Navier-Stokes equation, making numerical methods the primary means of solving them [1, 2]. Although these methods are effective, they are computationally expensive and often require significant computing resources. Classical numerical methods often require some trade-off in accuracy while pursuing computational efficiency. Therefore, there is an urgent need to find a class of efficient solution methods.

In recent years, deep learning researchers have made significant progress, making it possible for AI to replace traditional numerical solvers and numerical simulators [3, 4, 5, 6]. Notably, the concept of neural operators and their innovative architectures have demonstrated considerable promise in approximating intricate mappings, with extensive research conducted in this area. This paradigm aims to approximate the mapping relationship between inputs and outputs by training deep models with innovative architectures. Specifically, it learns correlations in time series data. For example, predicting future flows and pressures based on information about flows and pressures at a point in time in the past [7]. In addition, the method is capable of directly learning the mapping relationship between different parameters. For example, the macroscopic mechanical properties of a composite are inferred from its microstructure [8]. This approach has shown exceptional performance in various fields, including fluid mechanics and material mechanics.

Fourier neural operators have proposed a novel solution that performs well in handling partial differential equation (PDE) problems. It transforms the data into the Fourier domain for learning [9]. However, Fourier neural operators rely on the iterative update strategy of the operator, which can result in partial information loss during iterative calls. The main reason for this error accumulation is the frequent conversion between the spatial and spectral domains within different operational blocks, as well as negative multiplications performed inside the Fourier domain. In this process, some spatial information is lost due to the forward and backward transformations of spectral convolution. Therefore, the cumulative loss of spatial information in processing the same information after each iteration reduces its efficiency [10, 11].

The research in this paper focuses on developing a new operator architecture. The architecture uses Fast Fourier Transform (FFT) to learn partial differential equations. However, it solves the iterative error problem by using a clean and efficient parallel architecture. Our contributions are as follows:

- We propose a new neural operator architecture, the Deep Parallel Neural Operator. The overall architecture maps the raw data to different potential spaces after multiple encodings.
- We design a parallel operator block. It learns the input and output mappings of different potential spaces in parallel.
- We conduct six benchmark experiments to compare our model with benchmark models and currently recognized state-of-the-art models. Our model achieves the best results on five datasets with an average improvement of 10.5%, and ranks second on one dataset. In addition, we conduct an ablation study to compare the performance of parallel block with serial block. The results show an average performance improvement of 9.3% for parallel block.

2. Related work

2.1. Neural operator

Neural operators are a series of methods for learning meshless, infinite-dimensional operators using neural networks that have been proposed in recent years of research. Neural operators solve the mesh dependence problem of finite-dimensional operator methods by generating a set of mesh parameters that can be used for different discretisations [12]. It has the ability to transfer solutions between arbitrary meshes. In addition, the neural operator needs to be trained only once, and the subsequent performances of various new instance parameters require only forward propagation calculations. This reduces the computational cost associated with repeated training. Neural operators are purely data-driven and do not rely on any prior knowledge about partial differential equations [13]. This makes it possible for the operator to learn solutions to partial differential equations.

Specifically, neural operators are described as an iterative update architecture: $v_0 \rightarrow v_1 \rightarrow \cdots \rightarrow v_T$, Where v_j is a series of functions on \mathbb{R}^{d_v} . Input $a \in A$ is first elevated to a higher dimensional representation through local transformation P : $v_0(x) = P(a(x))$. This local transformation is typically

parameterized by a shallow fully connected neural network. Then apply several updates and iterations: $v_t \rightarrow v_{t+1}$. The output $u(x) = Q(v_T(x))$ is the projection of v_T through local transformation $Q: \mathbb{R}^{d_v} \rightarrow \mathbb{R}^{d_u}$. Each iteration of $v_t \rightarrow v_{t+1}$ is defined as a combination of non-local integration operator \mathcal{G} and local nonlinear activation function σ . Among them, the local integration operator is formalized as:

$$(G(a; \emptyset)v_t)(x) = \int_D \mathcal{K}(x, y, a(x), a(y); \emptyset)v_t(y) dy \quad \forall x \in D \quad (1)$$

where D represents the domain of the function, \mathcal{K} represents the kernel integral operator, parameterized by \emptyset .

2.2. Fourier transform and Fourier neural operator

Fourier transform is a mathematical transformation. It analyzes the frequency components of a signal by decomposing it into a combination of sine and cosine waves of different frequencies, and has wide applications in many scientific and engineering fields [14, 15, 16]. In practice, it is a spectral method commonly used to solve partial differential equations [17, 18]. The specific Fourier transform and its inverse transform form are as follows:

$$F(\omega) = \int_{-\infty}^{\infty} f(t)e^{-j\omega t} dt, \quad (2)$$

$$f(t) = \frac{1}{2\pi} \int_{-\infty}^{\infty} F(\omega)e^{j\omega t} d\omega. \quad (3)$$

In the Fourier domain, differential operations become simpler because differentiation is equivalent to multiplication in the Fourier domain. This makes Fourier transform a powerful tool for solving partial differential equations (PDEs), especially in cases involving frequency components. Through Fourier transform, complex differential equations can be transformed into algebraic equations that are easier to handle, thereby simplifying the solving process. Fourier transform has played an important role in the development of deep learning. In theory, Fourier transform appears in the proof of the general approximation theorem, which states that multi-layer neural networks can approximate any continuous function [19]. In practice, they are often used to accelerate convolutional neural networks [20]. Neural network architectures associated with Fourier transforms or sinusoidal activation functions are proposed and studied [21, 22, 23].

Recently, some spectral methods for partial differential equations have been extended to neural networks. A new neural operator architecture has been proposed by Li et al [7]. This architecture directly defines a kernel integration operator in Fourier space with quasi-linear time complexity and advanced approximation capabilities. This advancement opens new avenues for the application of neural networks in meshless and infinite dimensional spaces, thus enabling neural networks to efficiently handle complex partial differential equation problems.

The convolution operator is introduced in FNO to replace the kernel integration operator in Equation 1, Let F denote the Fourier transform of a function $f : D \rightarrow \mathbb{R}^d$, and F^{-1} its inverse, then

$$(\mathcal{F}f)_j(k) = \int_{-D}^D f_j(x) e^{-2\pi i x k} dx \quad (4)$$

And the inverse Fourier transform is given by:

$$(\mathcal{F}^{-1}f)_j(x) = \int_{-D}^D f_j(k) e^{2\pi i x k} dk \quad (5)$$

By specifying $k(x, y, a(x), a(y)) = k(x, y)$, and applying the convolution theorem, the Fourier kernel integral operator can be obtained:

$$K(\phi)v_t(x) = \mathcal{F}^{-1}(\mathcal{R}_\phi \cdot (\mathcal{F}v_t)(x)) \quad (6)$$

2.3. Operator-learning methods

In the study of various partial differential equation problems, numerous operator design schemes have been proposed, yielding good results. Most operator-learning methods utilize convolutional neural networks and fully connected neural networks [24, 25, 26]. DeepONet, developed by Lu et al. [27], is based on the universal approximation theorem. The network comprises two parts, a branch network and a trunk network, which process the information from the sampled points of the input function and the target points, respectively. The outputs of these two parts are then combined to generate the final result, effectively approximating and predicting complex nonlinear operators. Geo-FNO works by transforming complex geometric tasks such as point clouds into a potentially unified mesh. Use this mesh as an input to FNO to efficiently process complex geometries [28]. F-FNO introduces new separable spectral layers and improved residual connections,

combined with training strategies such as the Markov assumption, Gaussian noise, and cosine learning rate decay, significantly reducing errors on several benchmark PDEs [29]. MWT proposes a data-driven method for learning operator mappings by compressing operator kernels onto multi wavelet polynomial bases, utilizing the fine-grained representation of multi wavelet transforms and the properties of orthogonal polynomial bases [30]. SNO converts inputs and outputs into coefficients of basis functions, learning the mapping between inputs and outputs sequentially while alleviating systematic bias caused by aliasing errors [31]. KNO, based on Koopman theory, improves the performance of FNO in long-term predictions [32].

In addition, there are other operator methods with deep architecture designs. Based on the U-Net concept and residual connections, multi-scale processing is performed for PDE tasks [33, 34]. For example, U-NO’s U-shaped structure improves model depth and memory efficiency. In benchmark tests for solving partial differential equations, such as Darcy’s and Navestock’s equations, U-NO significantly improves prediction accuracy [35]. U-FNO enhances the ability of FNO to handle multi-scale data by using residual connections [36]. LSM proposes a projection technique that sequentially projects high-dimensional data into multiple compact latent spaces, thereby eliminating redundant coordinate information. Based on triangular basis operators, LSM decomposes complex nonlinear operators into multiple basis operators through neural spectral blocks, thereby improving the ability to solve complex partial differential equations [37]. These novel neural operator learning methods have made significant advances and breakthroughs in different fields, demonstrating excellent performance.

3. Method

3.1. Overall architecture

Current mainstream neural operators usually adopt an iterative update strategy, which leads to the problem of spatial information loss due to iteration. To address this problem, we propose a parallel architecture based on hierarchical projection called Deep Parallel Neural Operator (DPNO). This approach maps the data to different latent spaces, approximates the complex mapping between these latent spaces, and thus fits the overall input-output mapping. We use several simple and efficient parallel operator blocks to learn the mapping relations within different latent spaces, by employing different

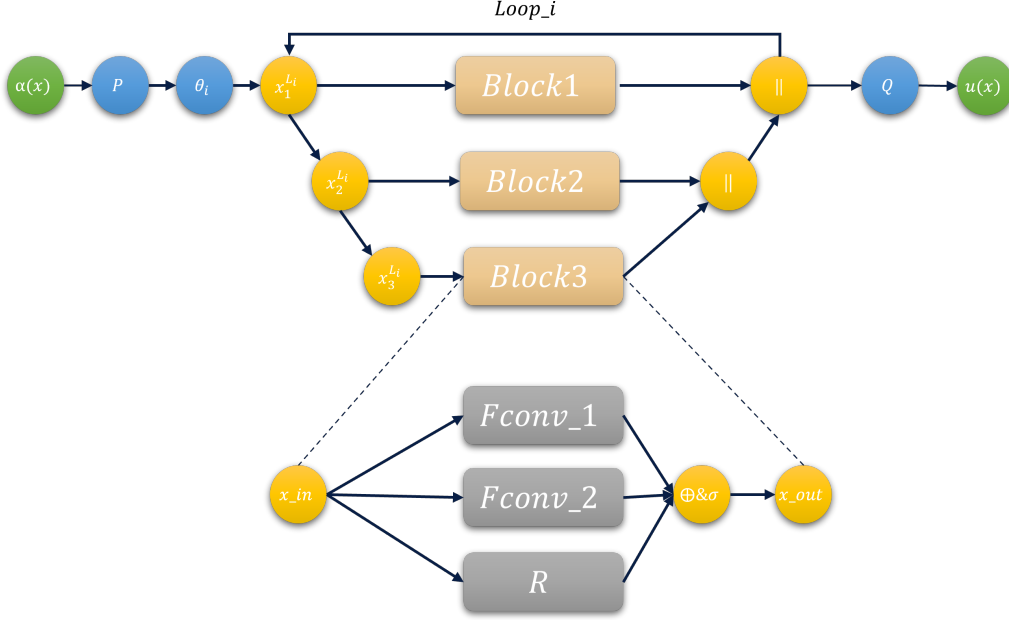


Figure 1: DPNO overall architecture

combinations of modal truncations to deal with different frequency information.

Overall architecture: Our model first maps data to different latent spaces through encoding, solves partial differential equations in multiple latent spaces, and finally returns to the original space through a decoder, as shown in fig 1. Specifically, the DPNO architecture is divided into three main modules:

$$G_\theta = \text{Loop} \left(G_{\theta_{\text{toLatentSpace}}} \circ G_{\theta_{\text{Ksolve}}} \circ G_{\theta_{\text{toOriginalSpace}}} \right) \quad (7)$$

where \circ denotes the sequential combination between operations. In the DPNO architecture, $G_{\theta_{\text{toLatentSpace}}}$ denotes encoding data and mapping it to different latent spaces, and decoding $G_{\theta_{\text{toOriginalSpace}}}$ projects the data from latent space to original space. $G_{\theta_{\text{Ksolve}}}$ denotes a complex mapping that approximates inputs and outputs from latent space to different subspaces. The term “Loop” denotes a Loop. To improve model efficiency and reduce the number of parameters, $G_{\theta_{\text{Ksolve}}}$ shares the same set of parameters in the loop and learns the same set of parameters twice, i.e., the loop iterates twice.

3.2. Encoder

The data preprocessing of this architecture is consistent with the previous standard components for neural operators. Given an input function $a : \mathcal{D}_A \rightarrow \mathbb{R}^{d_A}$, first perform a dimensionality increase operation P on a to calculate $v_0 : \mathcal{D}_A \rightarrow \mathbb{R}^{d_0}$, where the dimensionality increase operation P is parameterized by a shallow fully connected neural network, and its function is as follows:

$$v_0(x) = P(a(x)) \quad \forall x \in \mathcal{D}_0 \quad (8)$$

where $d_0 \gg d_A$. Then, through a local transformation ϕ_i :

$$x_1^{(L_i)} = \phi_i(v_0(x)) \quad i = 0, 1, \dots, T-1 \quad (9)$$

After the local transformations, the data are sequentially mapped to multiple potential spaces through a coding network.

The coding network is a central part of DPNO. It maps data sequentially to multiple compact potential spatial representations. Consider that the Fourier transform is globally valid. Unlike simple downsampling methods, projection networks use classical convolutional combinations to extract local information from the data. Features are downsampled and compressed through pooling operations as a way to map to a lower dimensional space. This combination not only preserves key spatial information in the data, but also removes redundant noise. As a result, the effectiveness and expressiveness of the data representation can be enhanced while reducing the dimensionality. For the given input $x_1^{(L_i)}$, the projection calculation is performed to obtain $x_2^{(L_i)} : \mathcal{D}_0 \rightarrow \mathcal{D}_1$. The combinatorial process is formally described as:

$$x_2^{(L_i)} = T(x_1^{(L_i)}), \quad x_3^{(L_i)} = T(x_2^{(L_i)}) \quad (10)$$

Where i represents the potential space number. In our model, we map the data to three different latent spaces that contain the original space. Two sets of representations in different latent spaces are obtained by two local transformations ϕ_i . These two local transformations are learnt using the same set of learnable parameter operators and projected using different learnable parameter encoding networks.

3.3. Parallel operator block and Decoder

With a hierarchical projection network, we map the data to different potential spaces. We use a parallel dual Fourier neural operator to approximate

the complex mapping between inputs and outputs. And a simple linear layer is used for residual connectivity to compensate for the loss of high-frequency information. The formal description is as follows:

$$G_{\theta_K} = \sum_{i=1}^N (W_{\theta_1}^i G_1^i, W_{\theta_2}^i G_2^i, R^i) \quad (11)$$

where i represents the potential space number. G_1^i and G_2^i respectively represent two parallel operators in the same latent space \mathcal{D}_i , each with learnable parameters $W_{\theta_1}^i$ and $W_{\theta_2}^i$. R^i is a simple linear network. Considering the frequency aliasing caused by coding, we employ a modal grouping strategy for modal truncation in different latent spaces. Specifically, the lower the spatial dimension, the smaller the modes are, thus adapting to the frequency information aliasing error. Different modes are used to extract different Fourier blocks in the same latent space. This is because low frequency information tends to retain more physical information.

$$G_{\theta_{\text{toOriginalSpace}}} : v_{\text{out}}^i(\mathbb{R}^{d^i}) \rightarrow v_{\text{out}}^{(i')}(\mathbb{R}^{d^{(i-1)}}), \quad v_{\text{out}}^{(i-1)}(\mathbb{R}^{d^{(i-1)}}) = [v_{\text{out}}^{(i')}, v_{\text{out}}^{(i-1)}] \quad (12)$$

The operation $v_{\text{out}}^i(\mathbb{R}^{d^i}) \rightarrow v_{\text{out}}^{(i')}(\mathbb{R}^{d^{(i-1)}})$ represents projecting the i -th latent spatial data to the $i - 1$ space through an ascending dimensional network. Merge $v_{\text{out}}^{(i')}$ with the outputs v_{out}^{i-1} of $i - 1$ spaces. Conduct merging of adjacent latent space outputs in a sequential manner until the process returns to the original space \mathbb{R}^{d_0} .

4. Experiment and results

4.1. Dataset and Experimental setup

In order to fully assess the performance of the model, we selected six partial differential equation benchmark datasets. The model relative errors were recorded. The selected benchmark datasets include typical partial differential equations in solid state physics and fluid physics and contain samples of different geometries. Details are given in Table 1.

Table 1: Benchmark dataset.

Physics	Benchmark	Geometry	#DIM
SOLID	Elasticity-G	Regular Grid	2D
SOLID	Plasticity	Structured Mesh	3D
FLUID	Navier-Stokes	Regular Grid	2D
FLUID	Darcy	Regular Grid	2D
FLUID	Airfoil	Structured Mesh	2D
FLUID	Pipe	Structured Mesh	2D

4.1.1. Navier-stokes equation

The Navier Stokes equation is a fundamental equation that describes fluid motion. For viscous and incompressible fluids, we consider the famous Navier Stokes equation as a two-dimensional problem. The general form of the Navier Stokes momentum equation with periodic boundary conditions on a unit torus $[0,1]$ is as follows:

$$\begin{aligned}
\frac{\partial u}{\partial t} + u \cdot \nabla u + \nabla p &= \nu \Delta u + f(x), \quad x \in T^2, \quad t \in (0, \infty) \\
\nabla u(x, t) &= 0, \quad x \in T^2, \quad t \in [0, \infty) \\
u(x, 0) &= u_0(x), \quad x \in T^2
\end{aligned} \tag{13}$$

Where ν is the fixed viscosity, u denotes the velocity, p is the pressure, and f is the external force function. The dataset is provided by the baseline model, and we used data with a grid resolution of 64×64 for both training and testing.

4.1.2. Plastic problem

Consider the plastic forming problem in which a block of material $\Omega = [0, L] \times [0, H]$ is subjected to the impact of a frictionless rigid mould at time $t = 0$. The mould is geometrically parameterised by an arbitrary function $S_d \in H^1([0, L]; \mathbb{R})$ and moves with a constant velocity v . The lower edge of the block of material is clamped and the upper edge is subjected to a displacement boundary condition. The lower edge of the material block is clamped and a displacement boundary condition is imposed on the upper

edge. The elastic-plastic intrinsic model is used in this case as follows:

$$\begin{aligned}\sigma &= C : (\epsilon - \epsilon_p), \\ \dot{\epsilon}_p &= \lambda \nabla \sigma f(\sigma), \\ f(\sigma) &= \begin{cases} \sqrt{3}|\sigma - \frac{1}{3}\text{tr}(\sigma) \cdot I|F - \sigma_Y & \text{if } \lambda \geq 0, f(\sigma) \leq 0, \lambda \cdot f(\sigma) = 0, \\ 0 & \text{otherwise.} \end{cases} \end{aligned} \quad (14)$$

where the plastic multiplier is constrained by $\lambda \geq 0$, $f(\sigma) \leq 0$, and $\lambda \cdot f(\sigma) = 0$. The isotropic stiffness tensor C is characterized with Young's modulus $E = 200$ GPa and Poisson's ratio $\nu = 0.3$. The yield strength σ_Y is set to 70 MPa with the mass density $\rho_s = 7850$ kg/m³.

The dataset is from the baseline model geo-FNO. Contains 980 training data and 80 test data. All data points are contained on a 101×31 structured grid with 20 time steps.

4.1.3. Other datasets

Other datasets include the Darcy flow problem, the elastic problem, the airfoil problem for the euler equations, and the pipe problem for the Navier-Stokes equations. Darcy flow problem, We consider the steady state of the two-dimensional Darcy flow equation in the unit rectangle. This is a second order linear elliptic partial differential equation with Dirichlet boundary conditions experiments are performed using a fixed resolution of $85 * 85$. The elastic problem is a solid domain problem where the input is mesh information and the target output is the corresponding stress field. The airfoil problem with Euler equations describes the flow characteristics of compressible air around a wing. The inputs are mesh point and Mach number information and the output is the Mach number. The pipe problem using the Navier-Stokes equations describes the flow of an incompressible fluid through a pipe. Inputs include grid point locations and horizontal velocities, and output data include velocity vectors and pressures. The above dataset is provided by the baseline model and consists of one solid-related problem and three fluid-related problems.

4.1.4. Baselines and Settings

In order to better demonstrate the performance of our proposed model, we compare DPNO with seven currently recognized state-of-the-art models, including U-Net, FNO, WMT, U-FNO, UNO, F-FNO, and LSM. Among them, LSM is currently the best overall performer on the six datasets. We

Table 2: Comparison of L2 errors for the 7 benchmark models on the 6 benchmark datasets. The best performing models are in bold, and the next best models are underlined.

Model	Pipe	Airfoil	Elastic-G	Plasticity	Darcy	NS
U-Net(2015)	0.0065	0.0079	0.0531	0.0051	0.0080	0.1982
geo-FNO(2019)	0.0067	0.0138	0.0508	0.0074	0.0108	0.1556
WMT(2021)	0.0077	0.0075	0.0520	0.0076	0.0082	0.1541
U-NO(2022)	0.0100	0.0078	0.0469	0.0034	0.0183	0.1731
U-FNO(2021)	0.0056	0.0269	0.0480	0.0039	0.0183	0.2231
F-FNO(2023)	0.0070	0.0078	0.0475	0.0047	0.0077	0.2322
LSM(2023)	0.0050	0.0059	0.0408	0.0025	0.0065	0.1535
DPNO	0.0052(-3.8%)	0.0054(8.5%)	0.0375(8%)	0.0019(24%)	0.0062(4.6%)	0.1418(7.6%)

used the same experimental setup for all models. The ADAM optimizer was used for all methods, with an initial learning rate of 10^{-3} for L2 loss and 501 training sessions. The batch size was set to 20.

4.2. Results and Discussion

DPNO achieved state-of-the-art performance on five benchmark datasets and one sub-optimal. An average improvement of 10.5% is achieved compared to the overall best performing LSM. This demonstrates the versatility and excellent performance of the proposed DPNO in different PDE tasks. Compared to the baseline model FNO, DPNO shows an average performance improvement of 39% on the six datasets. Among them, the performance of the PLAYCITY-3d problem is improved by 74%. As shown in table 2:

The experimental results are visualised in Figures 2-4:

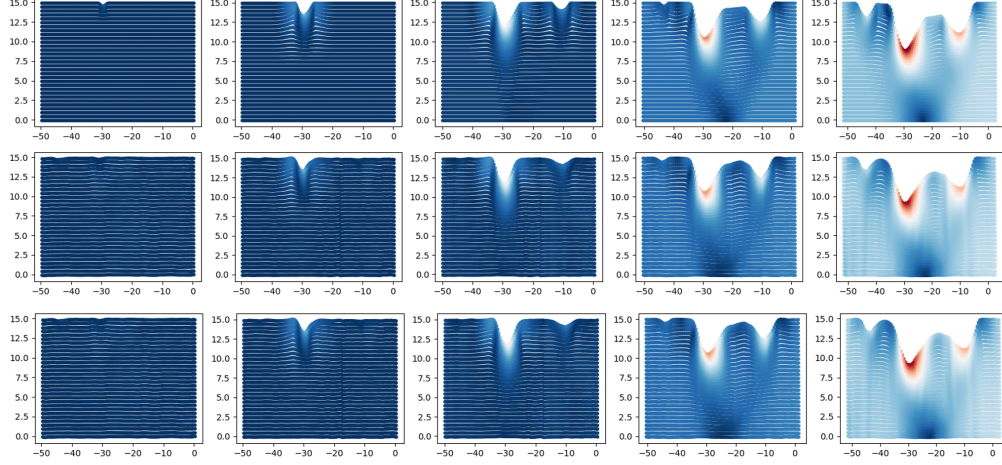


Figure 2: Plastic Problem: The top represents the true value, the middle represents the DPNO prediction, and the bottom line represents the FNO prediction. The five columns represent time variations. Colours represent displacement criteria.

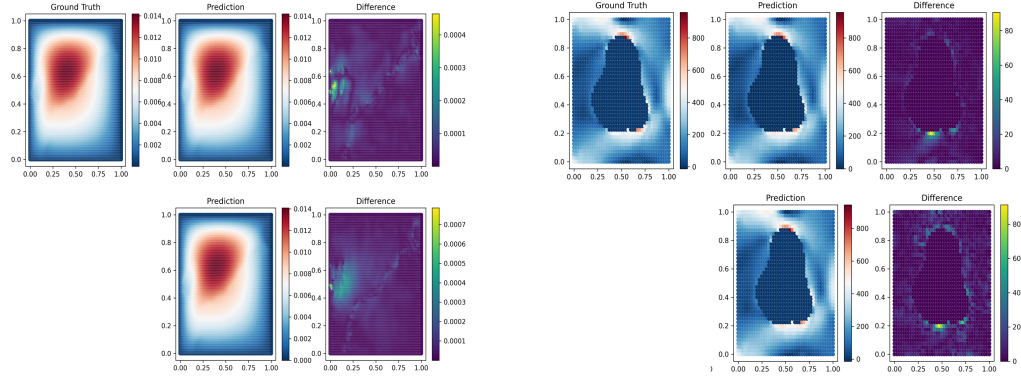


Figure 3: Darcy Flow Problem(left) and Elastic Problem(right): true values on the left, in the middle are the predicted values and errors for DPNO (top) and FNO (bottom)

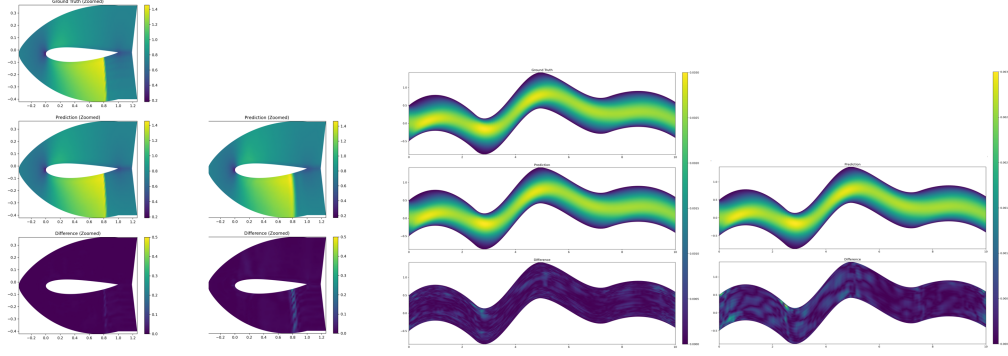


Figure 4: Airfoil(left) and Pipe Problem(right): top is the true value, middle and bottom are the predicted value and error for DPNO (left) and FNO (right) respectively.

4.3. Ablation experiment

In order to verify the effectiveness of the parallel strategy in the model, we design a set of ablation experiments to change the parallel block into serial block and observe the performance changes. Specifically, we merge the parallel block horizontally into serial block as shown in Fig.5.

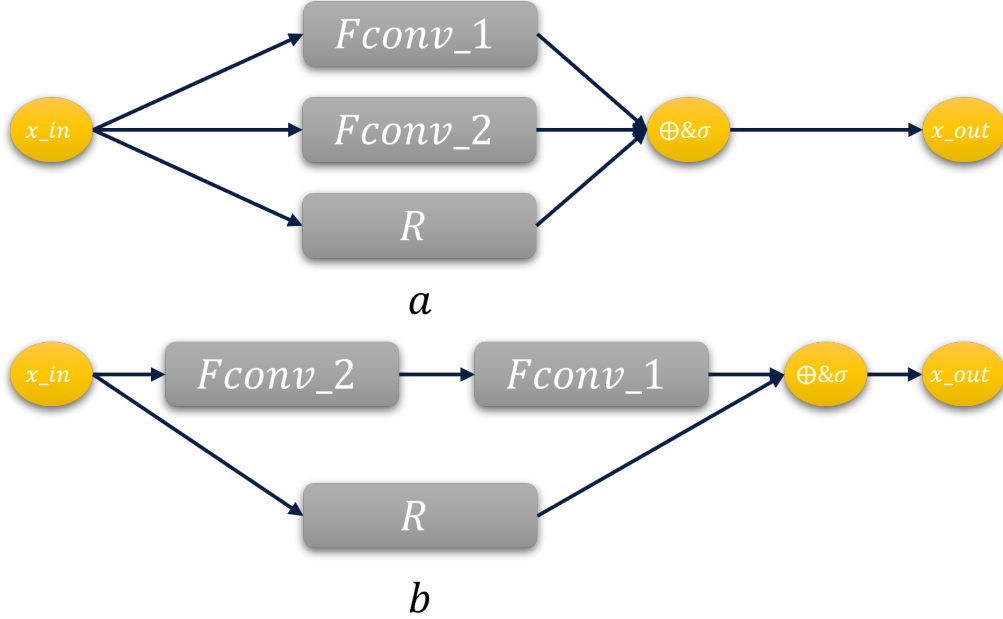


Figure 5: Parallel operator block (a) and serial operator block (b).

Table 3: Comparison of L2 errors for DPNO/P and DPNO on the 6 benchmark datasets. The improvement percentage is included in the DPNO row.

Model	Pipe	Airfoil	Elasticity-G	Plasticity	Darcy	NS	Total
DPNO/P	0.0059	0.0061	0.0384	0.0021	0.0069	0.1586	-
DPNO	0.0052	0.0054	0.0375	0.0019	0.0062	0.1418	9.3%

The experimental results are shown in Table 3:

Through the ablation experiments, we can find that parallelisation has some degree of impact on the overall model performance, with an average performance improvement of 9.3%. This is because by parallelising the module, we mitigate the error accumulation caused by the iterations.

5. Conclusions

Neural operators are good learners when it comes to functional spaces. In this paper, we propose a deeply parallel Fourier neural operator to address the problem of error accumulation during FNO iterations. Firstly, the data are projected into various potential spaces and learnt in an end-to-end manner through multiple parallel operator blocks. Excellent performance is achieved on six benchmark datasets for partial differential equations. An average improvement of 39% is achieved compared to the baseline model FNO.

Although the field of deep learning currently has good progress in learning partial differential equations. However, there are still shortcomings in long time prediction. The time dependence cannot be captured better. For dynamically changing systems, deep learning models may need to be constantly updated and retrained to adapt to new conditions.

References

- [1] Gockenbach M S, *Partial differential equations: analytical and numerical methods*, Society for Industrial and Applied Mathematics, 2010.
- [2] Tanabe H, *Functional analytic methods for partial differential equations*, CRC Press, 2017.
- [3] Raissi, M., Perdikaris, P., Karniadakis, G. E., *Physics-informed neural networks: A deep learning framework for solving forward and inverse problems involving nonlinear partial differential equations*, Journal of Computational Physics, 378, 686-707, 2019.

- [4] Jiang, C. M., Esmailzadeh, S., Azizzadenesheli, K., Kashinath, K., Mustafa, M., Tchelepi, H. A., Marcus, P., Anandkumar, A., et al., *Mesh-freeFlowNet: A physics-constrained deep continuous space-time super-resolution framework*, arXiv preprint, arXiv:2005.01463, 2020.
- [5] Greenfeld, D., Galun, M., Basri, R., Yavneh, I., Kimmel, R., *Learning to optimize multigrid PDE solvers*, In International Conference on Machine Learning, PMLR, 2019, pp. 2415–2423.
- [6] Kochkov, D., Smith, J. A., Alieva, A., Wang, Q., Brenner, M. P., Hoyer, S., *Machine learning accelerated computational fluid dynamics*, arXiv preprint, arXiv:2102.01010, 2021.
- [7] Li, Z., Kovachki, N., Azizzadenesheli, K., Liu, B., Bhattacharya, K., Stuart, A., Anandkumar, A., *Fourier neural operator for parametric partial differential equations*, arXiv preprint arXiv:2010.08895, 2020.
- [8] Lim, B., Zohren, S., *Time-series forecasting with deep learning: A survey*, Philosophical Transactions of the Royal Society A: Mathematical, Physical and Engineering Sciences, 379(2194), 2021.
- [9] He, Q., Xu, W., Zhang, T., *Composite materials microstructure–property modeling using machine learning*, Advanced Materials, 33(50), 2104146, 2021.
- [10] Boyd, J. P., *Chebyshev and Fourier Spectral Methods*, Dover Publications, 2000.
- [11] Rafiq, M., Rafiq, G., Jung, H. Y., et al., *SSNO: Spatio-spectral neural operator for functional space learning of partial differential equations*, IEEE Access, 2022, 10: 15084-15095
- [12] Li, Z., Kovachki, N., Azizzadenesheli, K., et al., *Neural operator: Graph kernel network for partial differential equations*, arXiv preprint, arXiv:2003.03485, 2020.
- [13] Kovachki, N., Li, Z., Liu, B., et al., *Neural operator: Learning maps between function spaces with applications to PDEs*, Journal of Machine Learning Research, 2023, 24(89): 1-97.

- [14] Kar, C., Mohanty, A. R., *Vibration and current transient monitoring for gearbox fault detection using multiresolution Fourier transform*, Journal of Sound and Vibration, 2008, 311(1-2): 109-132.
- [15] Sandryhaila, A., Moura, J. M. F., *Discrete signal processing on graphs: Graph Fourier transform*, in Proceedings of the 2013 IEEE International Conference on Acoustics, Speech and Signal Processing, IEEE, 2013, pp. 6167-6170.
- [16] Candès, E. J., Romberg, J., Tao, T., *Robust uncertainty principles: Exact signal reconstruction from highly incomplete frequency information*, IEEE Transactions on Information Theory, 2006, 52(2): 489-509.
- [17] Canuto, C., *Spectral Methods: Evolution to Complex Geometries and Applications to Fluid Dynamics*, Springer-Verlag, 2007.
- [18] Boyd, J. P., *Chebyshev and Fourier Spectral Methods*, Courier Corporation, 2001.
- [19] Hornik, K., Stinchcombe, M., White, H., et al., *Multilayer feedforward networks are universal approximators*, Neural Networks, 2(5):359–366, 1989.
- [20] Mathieu, M., Henaff, M., LeCun, Y., *Fast training of convolutional networks through FFTs*, 2013.
- [21] Bengio, Y., LeCun, Y., et al., *Scaling learning algorithms towards AI*, Large-scale Kernel Machines, 34(5):1–41, 2007.
- [22] Sitzmann, V., Martel, J. N. P., Bergman, A. W., Lindell, D. B., Wetzstein, G., *Implicit neural representations with periodic activation functions*, arXiv preprint, arXiv:2006.09661, 2020.
- [23] Mingo, L., Aslanyan, L., Castellanos, J., Diaz, M., Riazanov, V., *Fourier neural networks: An approach with sinusoidal activation functions*, 2004.
- [24] Krizhevsky, A., Sutskever, I., Hinton, G. E., *ImageNet classification with deep convolutional neural networks*, Advances in Neural Information Processing Systems, 2012, 25.

- [25] He, K., Zhang, X., Ren, S., Sun, J., *Deep residual learning for image recognition*, In *Proceedings of the IEEE Conference on Computer Vision and Pattern Recognition*, 2016, pp. 770-778.
- [26] Hinton, G., Deng, L., Yu, D., et al., *Deep neural networks for acoustic modeling in speech recognition: The shared views of four research groups*, *IEEE Signal Processing Magazine*, 29(6), 82-97, 2012.
- [27] Lu, L., Jin, P., Karniadakis, G. E., *DeepONet: Learning nonlinear operators for identifying differential equations based on the universal approximation theorem of operators*, arXiv preprint, arXiv:1910.03193, 2019.
- [28] Li, Z., Huang, D. Z., Liu, B., et al., *Fourier neural operator with learned deformations for PDEs on general geometries*, *Journal of Machine Learning Research*, 24(388): 1-26, 2023.
- [29] Tran, A., Mathews, A., Xie, L., Ong, C. S., *Factorized Fourier neural operators*, In *ICLR*, 2023.
- [30] Gupta, G., Xiao, X., Bogdan, P., *Multiwavelet-based operator learning for differential equations*, In *NeurIPS*, 2021.
- [31] Fanaskov, V., Oseledets, I., *Spectral neural operators*, arXiv preprint, arXiv:2205.10573, 2022.
- [32] Xiong, W., Huang, X., Zhang, Z., Deng, R., Sun, P., Tian, Y., *Koopman neural operator as a mesh-free solver of non-linear partial differential equations*, arXiv preprint, arXiv:2301.10022, 2023a.
- [33] Ronneberger, O., Fischer, P., Brox, T., *U-net: Convolutional networks for biomedical image segmentation*, In *Medical Image Computing and Computer-Assisted Intervention–MICCAI 2015: 18th International Conference, Munich, Germany, October 5-9, 2015, Proceedings, Part III 18*, Springer International Publishing, 2015, pp. 234-241.
- [34] Szegedy, C., Ioffe, S., Vanhoucke, V., et al., *Inception-v4, inception-resnet and the impact of residual connections on learning*, In *Proceedings of the AAAI Conference on Artificial Intelligence*, 2017, 31(1).
- [35] Rahman, M. A., Ross, Z. E., Azizzadenesheli, K., *U-NO: U-shaped neural operators*, arXiv preprint, arXiv:2204.11127, 2022.

- [36] Wen, G., Li, Z.-Y., Azizzadenesheli, K., Anandkumar, A., Benson, S. M., *U-FNO - An enhanced Fourier neural operator based deep learning model for multiphase flow*, arXiv preprint, arXiv:2109.03697, 2021.
- [37] Wu, H., Hu, T., Luo, H., et al., *Solving high-dimensional PDEs with latent spectral models*, arXiv preprint, arXiv:2301.12664, 2023.